Plant Physiol. (1986) 82, 853–858
0032-0889/86/82/0853/06/$01.00/0

Spatial Distributions of Potassium, Solutes, and Their Deposition Rates in the Growth Zone of the Primary Corn Root[1]

Received for publication November 25, 1985 and in revised form July 21, 1986

WENDY KUHN SILK*, THEODORE C. HSIAO, ULRIKE DIEDENHOFEN, AND CHRISTINA MATSON
Department of Land, Air, and Water Resources, University of California, Davis, California 95616

ABSTRACT

Densities of osmoticum and potassium were measured as a function of distance from the tip of the primary root of *Zea mays* L. (cv WF9 × mo17). Millimeter segments were excised and analyzed for osmotic potential by a miniaturized freezing point depression technique, and for potassium by flame spectrophotometry. Local deposition rates were estimated from the continuity equation with values for density and growth velocity. Osmotic potential was uniform, −0.73 ± 0.05 megapascals, throughout the growth zone of well-watered roots. Osmoticum deposition rate was 260 μosmoles per gram fresh weight per hour. Potassium density fell from 117 micromoles per gram in the first mm region to 48 micromoles per gram at the base of the growth zone. Potassium deposition rates had a maximum of 29 micromoles per gram per hour at 3.5 millimeters from the tip and were positive (*i.e.* potassium was being added to the tissue) until 8 millimeters from the tip. The results are discussed in terms of ion relations of the growing zone and growth physics.

Recent theoretical work elucidates relationships between spatial and temporal patterns in growing tissue (20, 22). Two implications of the theoretical analyses are important for physiologists interested in ion and metabolite transport processes. First, to understand growth physiology and water relations, it is necessary to study the distribution of ions and solutes in growing tissue and on the temporal and spatial scales of the distribution of growth. To discover the physiological importance of ion and solute concentrations or deposition rates, the investigator must seek correlations between local growth rates and local concentrations of the substance of interest. Second, knowledge of the distribution of growth velocity (rate of displacement of cellular particles during growth) can add greatly to our understanding of developmental processes. In the context of ion and metabolite transport processes, the requirement for conservation of mass implies that local deposition rates can be evaluated if data on the distribution of growth velocity are combined with data on the density of the substance of interest. The experimental measurements are suggested by the continuity equation (20, 22–24):

$$D = \partial S/\partial t + \partial(Sv_z)/\partial z \quad (1)$$

where D represents the local deposition rate, S is the local density of substance S (solutes, K, or water), t is time, z is distance from the root tip, and v_z is local rate of displacement from the root apex.[2] Equation 1 confirms that deposition may occur even when the local density is unchanging in time, *i.e.* when the first term on the right hand side is negligible, and shows the importance of knowing the growth velocity.

Plant physiologists have long been interested in distributions of ions and ion uptake rates within plants, but most studies have focussed on nongrowing regions (17, 25) or on tissue segments which are large compared to the growth zone (9, 17, 26) or on uptake into excised tissue (2, 5, 25, 26). A few efforts have been made to characterize the distributions of K (11, 12, 16, 19) and osmotically active solutes (1, 3, 16) within growing regions. Characterization of osmoticum is relevant for models of growth which contain osmotic potential as an important driving force for growth-sustaining water uptake. Potassium is an important constituent of total osmotic concentration and, as an exchanger for hydrogen ions and/or a cofactor for ATPase activity, may be mechanistically related to growth. Here, we measure the distribution of potassium and total osmoticum and calculate net deposition rates of potassium and solutes in the primary root of maize, *Zea mays*, an organ for which the distribution of elongation growth is well characterized (4).

MATERIALS AND METHODS

Plant Cultivation. Seeds of *Zea mays* L. (cv WF9 × mo17) were surface sterilized for 5 min in commercial bleach ('Generic bleach,' Tracy Chemical Co.) diluted with 4 parts distilled H_2O and were germinated in vermiculite well moistened with 0.1 mM $CaCl_2$ for approximately 31 h at 29°C. Selected seedlings with terminal radicles about 7 mm long were transplanted to moist vermiculite wetted with 5 ml 0.1 mM $CaCl_2$ per g vermiculite in plexiglass boxes with one side slanted at 3 degrees from the vertical. Growth was at 29°C, and seedlings were kept in the dark except for exposure to dim light during marking. Between 17 and 18.5 h after transplanting, eight roots of uniform growth were selected and marked with india ink at approximately 1 mm increments for 12 mm. The criterion for uniformity was that total elongation rate be between 2.8 mm h^{-1} and 3.2 mm h^{-1} as measured by marking the position of root tips on the plexiglass surface at different times. After marking, roots grew undisturbed for 1 h, and then growth was analyzed by time lapse photography as described in (24). Computer assisted digitization of the marked photographs provided velocity profiles used in the continuity

[1] Supported by National Science Foundation grants PCM 8100296 and DCB 8417504 to W. K. S. and T. C. H.

[2] Definitions of symbols used as mathematical variables: D, local deposition rate (nmol mm^{-1} root length h^{-1} or μmol g^{-1} fresh weight h^{-1}); t, time (h); z, longitudinal coordinate, distance from root tip (mm); v_z, longitudinal growth velocity, rate of displacement from root tip (mm h^{-1}); $R(z)$, root radius at the location z mm from the tip (mm), ψ_s, osmotic potential (MPa); S, amount of substance (K, solutes, or water) found in 1 mm of root length (nmol mm^{-1} or mg mm^{-1}); L, total strain rate or local relative rate of volume increase (h^{-1}); L_z, longitudinal strain rate or relative elemental elongation rate (h^{-1}).

equation.

Device to Measure Osmotic Potential (ψ_s). Osmotic potential was measured cryoscopically. The approach of Marr and Vaadia (15) was modified to accommodate samples as small as a few microliters. The device used is shown in Figure 1. Melting point of a frozen sample was determined with a fine wire (76 μm diameter) T-type thermocouple wound around a brush bristle and glued with epoxy resin so that the wetted junction extended 0.5 mm beyond the end of the bristle. The wire and the bristle were led through a centered hole in a plexiglass rod and cemented to the end with epoxy. The rod was shaped to position the thermocouple junction in the center of the sample container, with the liquid surface below the rod (Fig. 1). The sample container was cut from an eye dropper or symmetric Pasteur pipette, with the small end sealed by fire polishing. The reference junction of the thermocouple was placed in a well insulated ice bath with at least 20 cm of the lead wire folded and immersed in the bath. The output of the thermocouple was amplified with a model 150 B microvolt meter (Keithley Instruments, Cleveland OH 44139). The sample with the thermocouple in place was quickly frozen by immersing the lower portions of the container with a rotary motion in a dry ice-methanol mixture. Controlled melting was then carried out by placing the lower two-thirds of the container in lubricating oil (used to provide a stable thermal medium at room temperature). Prior to immersion in oil, it was necessary to wipe dry the container quickly but thoroughly. Traces of methanol or ice formed from water vapor in the atmosphere on the outside of the container caused abrupt small changes in the recorder tracing. For very small sample volumes, the oil was cooled to slow down the thawing for a more distinct melting point. An example of the temperature recorder tracing is shown in Figure 1. As is conventional for cryoscopic determination of osmotic potential (15), freezing point was measured as the intersection of two straight lines, one drawn through the region of nearly constant temperature and the second drawn through the region of rapid temperature rise after thawing. The freezing point apparatus was calibrated using a series of standard sucrose solutions of known osmotic potentials. Voltage output was a linear function of osmotic potential. For six replicates on samples of equal ψ_s the standard error was ±0.05 MPa. The miniaturized freezing point apparatus requires larger sample size than some commercially available devices (Clifton Physics nanoliterosmometer) but it is more versatile in that it can measure

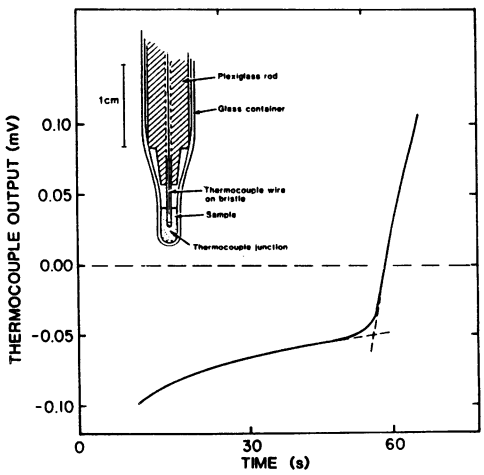

FIG. 1. Miniaturized freezing point depression apparatus (diagram) used to determine solute potential. Freezing point was determined from the inflection (intersection of dashed lines) in the experimental curve (solid line) of millivolt output *versus* time. The apparatus was calibrated with sucrose solutions of known solute potential as described in text.

ψ_s of tissue macerate as well as expressed cell sap.

Osmotic Potential and Potassium Content. For the determination of osmotic potential or K content, primary roots were harvested 18 h after transplanting, when they had attained a total length of about 5 cm. Seedlings were transferred to a humid chamber (near saturation humidity) and placed on moist, but not wet, paper towels. Adhering vermiculite was removed from the roots. A major part of the root cap was excised and discarded by making a transverse cut with a sharp razor blade 0.5 mm from the tip of the root cap at the junction of the root cap and apex. The root was then sectioned into 1-mm serial segments, starting at the root apex and ending at 12 mm, using scale markings on the paper towel or a jig made of 12 razor blades held rigidly between shims. (The two sectioning techniques gave identical results.) For subsequent computations the solute or K content of the segment extending from 0.5 to 1.5 mm was defined to be '*S*' at 1.0 mm, etc.

For the determination of osmotic potential, segments from 25 roots were combined, placed in a closed small volume container, frozen quickly on dry ice, transferred to the sample container of the freezing point apparatus, and partially thawed. The segments were macerated with a small glass rod, and the thermocouple was installed centrally in the macerate without removing the tissue debris. The melting point was determined after quick freezing.

For the determination of K content, seedlings were washed in 0.5 mM $CaSO_4$ and then rinsed in distilled H_2O. Collected 1-mm segments from about 20 roots were weighed, suspended in 5 cm^3 of 3% HNO_3 and heated to approximately 80°C for 2 h to extract K. The extract was adjusted to a final volume of 5 cm^3 and analyzed for K by flame photometry using a Beckman DU spectrophotometer. A series of standard solutions of KCl was run with each set of analyses.

Numerical Methods. Methods were adapted from Silk *et al.* (24). Total strain rate, L, a measure of the local relative rate of volume increases, was calculated as

$$L = \partial v_z/\partial z + (2/R)(v_z)(\partial R/\partial z) \quad (2)$$

where the first term on the right-hand side represents the local relative elongation rate and the second term represents the radial and tangential components of the relative growth rate (21). Erickson's five point and three-point differentiating formulas (4) were used to obtain derivatives of functions equally spaced in the abscissa. Cubic splines (Tektronix package) were used to interpolate nonequally spaced points to an equally spaced data set where necessary. Because the midpoint formulae were used, derivatives could be evaluated only between the second and second-to-last values of the abscissa. Deposition rates were calculated from Equation 1. Division by the fresh weight of the mm segment gave deposition rate per gram. Solute content of a 1-mm segment, [S], was estimated with the conventional formula (27):

$$S = -(\psi_s)(W)/RT \quad (3)$$

where W represents the volume of the water in the 1-mm segment (calculated from the difference between fresh weight and dry weight); R is the gas constant; and T is absolute temperature.

RESULTS

Distributions of Physical Properties and Growth Rate within the Growth Zone. To obtain information for subsequent calculations, roots were photographed (for measurement of diameter) and cut into mm segments which were weighed, dried, and reweighed. Average values of root radius, fresh weight, and dry weight were tabulated as functions of distance from the root tip (Table I). Compared to other seedling corn roots for which data

Table I. *Profiles of Physical Properties (Average Values Obtained as Described in Text)*

Distance From Tip	Radius	Fresh Weight	Dry Weight
mm		*mg mm^{-1}*	
1	0.34	0.50	0.069
2	0.43	0.76	0.111
3	0.53	0.93	0.114
4	0.58	1.01	0.086
5	0.62	0.99	0.079
6	0.62	1.03	0.072
7	0.64	1.05	0.065
8	0.65	1.06	0.069
9	0.67	1.04	0.065
10	0.68	1.08	0.069
11	0.68	0.98	0.065

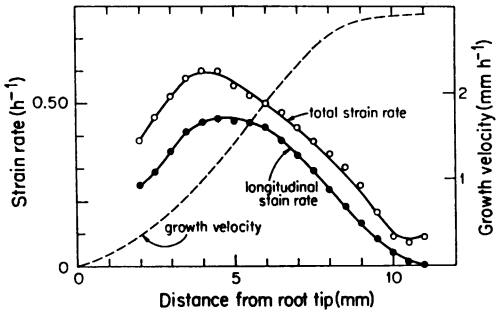

FIG. 2. Spatial distribution of growth. Growth velocity (rate of displacement from root tip, dashed line) increases with distance to a maximum of 2.9 mm h^{-1} at the base of the growth zone. Derivative of growth velocity with respect to position gives longitudinal strain rate (relative elemental rate of length increase, ●). Addition of a term for radial and tangential growth rate components yields the total strain rate (relative elemental rate of volume increase, ○) as shown in Equation 2.

have been reported (2, 4), the roots in this study were growing faster at a higher temperature and proved to be more conical.

Distributions of growth velocity (dashed line) and strain rate are shown in Figure 2. The longitudinal growth velocity and longitudinal strain rate ('relative elemental growth rate,' ●) are similar to those measured by Erickson and colleagues three decades ago (4). The distribution of the total strain rate has not previously been characterized. The total strain rate analysis shown in Figure 2 (○) reveals that the radial and tangential components contribute as much as one-third of total strain rate in the 2- to 4-mm region. The strain rate distributions provide the basic description of growth for comparison with distributions of solutes and solute deposition rates. The velocity profile was used with Equation 1 in calculations of deposition rates.

Osmotic Potential and Osmoticum Production Rate. Osmotic potential was uniform along the length of the root growing zone (Fig. 3, top). The magnitude of ψ_s varied somewhat among seed lots. In the seed lot studied here, ψ_s, determined from six replicate experiments, was 0.73 ± 0.050 MPa. Furthermore, ψ_s was approximately steady (time invariant), since values in young roots were within 0.05 MPa of values found in roots 10 h older (not shown). Roots which grew rapidly, 3.11 mm h^{-1}, had osmotic potentials which were indistinguishable from roots which had grown more slowly at 2.5 mm h^{-1} (not shown).

Because the osmotic potential was constant along the length of the growth zone, the solute content of a region, calculated on the basis of the volume of water in each mm segment, varied with the water content of the region. Figure 3 (bottom) shows

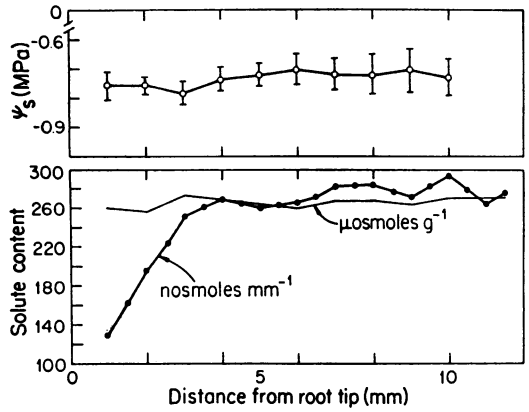

FIG. 3. Spatial distribution of solutes. (Top) Spatial distribution of solute potential. (Bottom) Solute density calculated from solute potential and expressed per unit root length (—●—) or per g fresh weight (——).

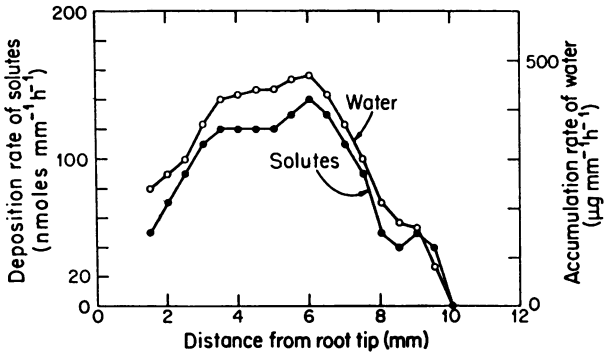

FIG. 4. Spatial distributions of solute deposition rate (●) and water accumulation rate (○).

that the solute content increases from 130 nosmol per mm of root length at z = 1 mm to 270 nosmol mm^{-1} at z = 4 mm. The increase per unit length is due to the increase in water content associated with widening of the root in the apical region, as indicated by the uniformity of osmoticum content per unit fresh weight, approximately 260 μosmol g^{-1}.

The uniformity of the osmotic potential profile also implies that osmoticum production rates must parallel the water accumulation rates. The calculated osmoticum deposition rates exhibited this expected trend (Fig. 4). The solute deposition rate rose from 50 nosmol mm^{-1} h^{-1} at z = 1.5 mm to 120 nosmol mm^{-1} h^{-1} at z = 4 mm while the water accumulation rate increases from 220 to 430 μg mm^{-1} h^{-1} over the same distance. Expressed per unit tissue weight, the osmoticum deposition rate was rather constant, approximately 120 μosmol g^{-1} h^{-1} over the 2- to 6-mm region (not shown). Expressed either gravimetrically or per unit root length, in the distal half of the growth zone the net solute deposition fell smoothly to a negligible rate at the base of the growth zone.

Potassium Density and Production Rate. The distribution of K differed from that of osmoticum in both spatial and temporal aspects. Expressed on a fresh weight basis, the concentrations showed a maximum in the first mm, where there were 117 μmol g^{-1}, and fell to 48 μmol g^{-1} at the end of the growth zone (Fig. 5). In contrast to the uniformity of the osmotic potential distribution, the K density exhibited a peak of 109 nmol mm^{-1} at 3 mm from the root tip and then declined smoothly to 60 nmol mm^{-1} beyond the elongation zone, at 12 mm from the tip (not shown). An implication of Figure 5 is that the elongating tissue elements lose K concentration as they are displaced; *i.e.* the gradient in K density, and hence the convective change in K

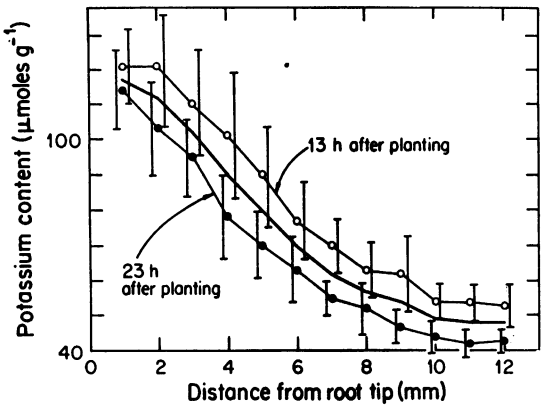

FIG. 5. Spatial distribution of K density in young roots (○) and roots 10 h older (●). Bars show SE for 7 sets of roots with 20 roots pooled per set. The average of these two curves (—) was used in calculating the last term in the equation for deposition rate. The difference between the two curves was used in evaluating the local rate of change, $\Delta s/\Delta t$.

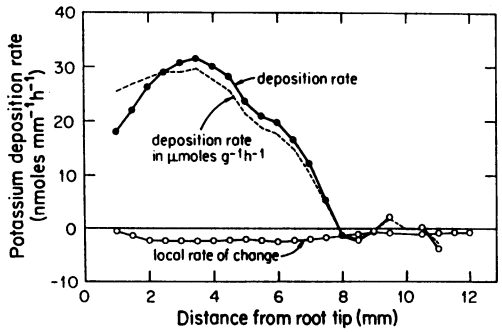

FIG. 6. Spatial distribution of K deposition rate, calculated per unit root length (●) or per gram fresh weight (- - - -). The local rate of change (○) proved numerically smaller than the growth velocity term of Equation 1.

density (22, 24), becomes negative. Another difference between the osmoticum and K distributions is that K content shows definite local decreases with age (Fig. 5). Roots harvested 13 h after planting had approximately 20 nmol mm^{-1} more K than roots harvested 23 h after planting. Thus local rates of change (embodied in the first of the two components of Equation 1) must be considered in calculation of K deposition rates (Fig. 6). Although the local changes in K content were large over a 10-h period, the local rates of change on an hourly basis, approximately 2 nmol mm^{-1} h^{-1}, proved smaller than the growth velocity term. Calculations indicated a net accumulation maximum of 32 nmol mm^{-1} h^{-1} at $z = 3.5$ mm and a net negative deposition rate, signifying local removal of K, starting at 8 mm behind the tip. Again because the root thickens with distance, the gravimetric deposition rate is high throughout the apical 4 mm. The peak deposition rate per gram fresh weight is 29 μmol g^{-1} h^{-1} at $z = 3.5$ mm.

Temporal Aspects. Elements of root tissue are displaced from the apex to the base of the growth zone and experience in a coordinated temporal sequence the densities and deposition rates shown as functions of position in Figures 3 to 6. The time scale is of interest and can be inferred by combining the previously published growth trajectory (plot of element position *versus* time) with the spatial pattern (10, 22). The resulting plot (Fig. 7) gives the deposition rate associated with a real or material (and infinitesimally small) tissue particle as it is displaced in time and space. Figure 7 is termed a 'Lagrangian specification' or a 'material specification' of the deposition rate because, in contrast to the spatial specifications of Figures 1 to 6, it refers to a tissue

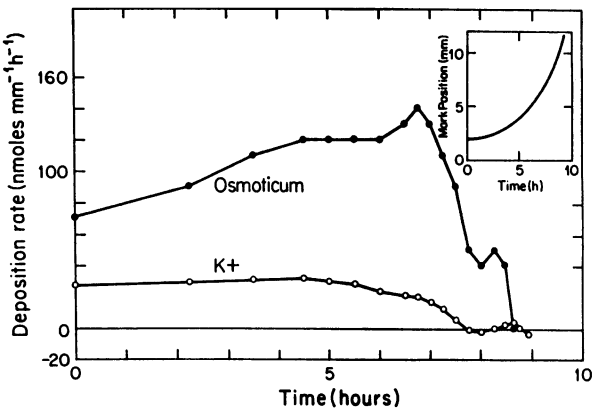

FIG. 7. Time course of deposition rates. A growth trajectory (plot of mark position *versus* time, inset) was used to find the time required for a particle to move from its initial position, 2 mm behind the apex, to more basal locations. Then the deposition rate associated with each location was obtained from Figure 4 or 6 and plotted against time. Unlike the other figures of this paper, this curve refers to the deposition rates associated with an individual (infinitesimally small) element of root tissue which is displaced in space and time.

particle (20, 22). The particle is identified initially 2 mm from the root tip and requires 4.5 h to move from 2 mm to 3 mm, where it has acquired the maximum K deposition rate, and only an additional 4.2 h for the rapid displacement through the basal part of the growth zone (Fig. 7). Deposition rates of both K and osmoticum can be seen to fall abruptly after 7 h of growth.

In interpreting the results of the figures one must realize that the time-dependent variables, including the deposition rates of Figures 4, 6, and 7, vary with the organ growth rate. The deposition rates of this study are probably close to maximum values for the corn root, because roots were growing at the temperature for maximum elongation rate. In contrast to the deposition rates the spatial profiles of solute and K density (Figs. 3 and 5) are less affected by temperature induced growth rate variation (not shown).

DISCUSSION

In this section we consider first the use and limitations of the continuity equation. Finally, we discuss the implications of the results shown in Figures 2 to 7 for growth physiology.

The deposition rate curves may be viewed as quantitative pictures of sink and source relationships. Regions of positive net deposition rate may be viewed as sink regions, while regions of negative net deposition rate are acting as sources, *i.e.* substance is being exported from them. Thus Figure 6 shows that in the corn roots of this study, the growing region apical to 8 mm is a sink for K^+. Others have shown (29) that $[K^+]$ continues to decrease with distance in the basal region behind the growth zone. In this region, where there is no strain rate component, a negative spatial gradient must mean a negative deposition rate (22, 24). Thus the region distal to 8 mm is providing K to the more apical tissue and/or to the external medium. This discussion demonstrates a limitation of Equation 1. The continuity equation calculations provide net local deposition rates but do not allow us to determine whether K deposition in the apical regions is exogenous, via uptake from the nutrient medium, or endogenous, via phloem unloading and plasmodesmatal transport. Uptake and efflux experiments using radioactive label might be used to answer this question. In the seedling root the endogenous source regions, drawing ultimately from the seed, must provide at least part of the K deposited in the sink regions. K is highly mobile in the phloem, and probably reaches growing

regions via phloem plus symplasmic transport (13). On the other hand, exchange with the external medium undoubtedly occurs (13).

A related question is whether the osmoticum deposition rate is produced by local degradation of stored polysaccharides and proteins or by import of osmotically active substances. Again, use of radioactive label has provided some answers. Giaquinta (8) has given convincing evidence that sucrose is supplied to the maize root tip from the seed via phloem and symplasmic transport.

In the extensive ion uptake literature we could find only one study with an approach similar to the one taken here. Scott *et al.* (19) inferred bean root growth velocities with an ingenious formula using cell lengths; they correctly combined growth data with data on density profiles of K and chloride to calculate the profile of ion deposition rates. It is instructive to compare Scott's formula to our Equation 1. Scott computes a variable ϕ the deposition rate per unit cell length, l of cortical tissue. If one recognizes that the material derivative of cell length is given by the product of displacement velocity and gradient in cell length, and that in the absence of cell division this equals the cell elongation rate evaluated as the product of longitudinal strain rate and existing cell length:

$$v_z(\partial l/\partial z) = l(\partial v_z/\partial z) \quad (4)$$

then it can be shown that

$$\phi = lD \quad (5)$$

i.e. multiplication of the local deposition rate of this study by cell length will give the material element deposition rate of Scott *et al.* This derivation illuminates the contrast between Figure 6, which indicates a smoothly falling K deposition rate in the distal half of the growth zone, and the conclusion by Brown and Cartwright (2) that "per cell, absorption [of K^+] increases as expansion occurs in the root." Since the K density declines to only half its maximum value during the growth period in which cell length increases more than eight fold, it is clear that the K content per cell increases more than 4-fold during growth.

To obtain insight into growth physiology we compare Figure 2 to Figures 3 to 6. Correlations are sought between magnitude of the local strain rate and putative causal agents of growth. The maintenance of a constant osmotic potential throughout the growth zone suggests that production of osmoticum is closely synchronized with growth in well-watered roots. Whether the strain rate is large (in the 4-mm region and in fast-growing roots) or small (in the 8-mm region and in more slowly growing roots), the well-watered roots have $\psi_s = -0.73$ MPa. A corollary is that osmoticum production *per se* does not cause the increase or decrease in the strain rate profile. From the literature it appears that this constancy of osmotic potential is not universal in growing tissue. Beck (1) showed solute concentration remains constant during growth of epidermal cells of sunflower hypocotyls. But when McNeil (16) examined entire cross-sections of this hypocotyl tissue, his data showed a drop in total solutes in the apical 2.5 cm which, from cell growth data, appear to comprise the growth zone. Others have also found that osmoticum becomes diluted during growth (3, 18). In contrast, solute density increases with distance from the tip in roots experiencing water stress (R Sharp, TC Hsiao, WK Silk, unpublished data). Studies of Cosgrove (3), Lockhart (14), and Van Volkenburgh and Cleland (28) have demonstrated the importance of wall extensibility in controlling stem and leaf growth rate. Taken together, the published data show that the rheological and/or metabolic properties of walls allow the cell to grow under a variety of osmotic potentials.

The $[K^+]$ profile of Figure 5 is similar to other K distributions which have been obtained in intact or freshly excised roots (11, 12, 19). The highest concentrations of K are always found near the root tip which corresponds to the youngest region. In leaves, too, K density is maximum in young leaves and decreases during the rapid expansion phase (6). In the corn root we see that the ion concentration maximum occurs near the region of maximum protein deposition rate (23). The K concentration in root meristems may be optimum for protein synthesis (7). Continuing to speculate about the relationships among the spatial distributions, we note that the maximum in gravimetric $[K^+]$ occurs apical to the region of maximum strain rate. This is consistent with a causal link between $[K^+]$ and elongation growth. Accumulating K ions could serve as counterions to promote hydrogen ion efflux and subsequent wall loosening. K could also stimulate membrane-bound ATPases to enhance its own uptake to promote growth. On the other hand, arguing against a simple involvement of K in controlling elongation rate, we note that both gravimetric $[K^+]$ and deposition rate have begun to fall by the 4-mm region, where strain rate begins its long plateau.

In general, the deposition rates of Figures 4 and 6 will appear different from profiles obtained in ion uptake experiments. To avoid artifacts produced by cell displacement during the label incubation period, uptake experiments to localize uptake rates must be performed on a time scale of 15 min (24). Yet many ions require more time than this to equilibrate with cellular compartments (24). Use of excised tissues can lower equilibration time but produces wounding effects and removes the normal supply of sugars and ions. The approach taken here, involving resolution of ion and solute density on the spatial scale of the growth rate distribution, adds to our understanding of growth physiology and permits calculation of the local deposition rates associated with the growth pattern.

LITERATURE CITED

1. BECK WA 1941 Production of solutes in growing epidermal cells. Plant Physiol 16: 637–642
2. BROWN R, PM CARTWRIGHT 1953 The absorption of potassium by cells in the apex of the root. J Exp Bot 4: 197–221
3. COSGROVE DJ 1985 Cell wall yield properties of growing tissue. Plant Physiol 78: 347–356
4. ERICKSON RO 1976 Modeling of plant growth. Annu Rev Plant Physiol 27: 407–34
5. ESHEL A, Y WAISEL 1973 Variations in uptake of sodium and rubidium along barley roots. Physiol Plant 28: 557–560
6. FREEMAN BL, WK KLIEWER 1984 Grapevine leaf development in relationship to potassium concentration and leaf dry weight and density. Am J Bot 71: 294–300
7. GIBSON TS, J SPEIRS, CJ BRADY 1984 Salt tolerance in plants. I. *In vitro* translation of mRNAs from salt-tolerant and salt-sensitive plants on the wheat germ ribosomes. Response to ions and compatible organic solutes. Plant Cell Environ 7: 579–587
8. GIAQUINTA RT 1979 Phloem loading of sucrose in corn roots. Plant Physiol 63: 744–748
9. HANSON JB, JS KAHN 1957 The kinetics of potassium accumulation by corn roots as a function of cell maturity. Plant Physiol 32: 497–498
10. HSIAO TC, WK SILK, J JING 1986 Leaf growth and water deficits: biophysical effects. *In* NR Baker, WJ Davies, CK Ong, eds, Control of Leaf Growth. Cambridge University Press, Cambridge, pp 239–266
11. JACOBSON L, R OVERSTREET 1947 A study of the mechanism of ion absorption by plant roots using radioactive elements. Am J Bot 34: 415–420
12. JESCHKE WD, W STELTER 1976 Measurement of longitudinal ion profiles in single roots of *Hordeum* and *Atriplex* by use of flameless atomic absorption spectroscopy. Planta 128: 107–112
13. LÄUCHLI A 1972 Translocation of inorganic solutes. Annu Rev Plant Physiol 23: 197–218
14. LOCHART JA 1965 An analysis of irreversible plant cell elongation. J Theor Biol 8: 264–75
15. MARR AG, Y VAADIA 1961 Rapid cryoscopic technique for measuring osmotic properties of drop size samples. Plant Physiol 36: 677–680
16. MCNEIL DL 1976 The basis of osmotic pressure maintenance during expansion growth in *Helianthus annuus* hypocotyls. Aust J Plant Physiol 3:311–324
17. PITMAN MG 1965 Sodium and potassium uptake by seedlings of *Hordeum vulgar.* Aust J Biol Sci 18: 10–24
18. RAYLE DL, R CLELAND 1972 The *in vitro* acid growth response: relation to *in vivo* growth response and auxin action. Planta 104: 282–296
19. SCOTT BIH, H GULLINE, CK PALLAGHY 1967 The electrochemical state of

cells of the broad bean roots. I. Investigation of elongating roots of young seedlings. Aust J Biol Sci 21: 185–200
20. SILK WK 1984 Quantitative descriptions of development. Annu Rev Plant Physiol 35: 479–518
21. SILK WK, S ABOU HAIDAR 1985 Growth of the stem of *Pharbitis nil*: analysis of longitudinal and radial components. Physiol Veg. 24: 109–116
22. SILK WK, RO ERICKSON 1979 Kinematics of plant growth. J. Theor Biol 76: 481–501
23. SILK WK, RO ERICKSON 1980 Local biosynthesis rates of cytoplasmic constituents in growing tissue. J Theor Biol 83: 701–703
24. SILK WK, RC WALKER, J LABAVITCH 1984 Uronide deposition rates in the primary root of *Zea mays*. Plant Physiol 74: 721–726
25. STEWARD FC, P PREVOT, JA HARRISON 1942 Absorption and accumulation of rubidium bromide by barley plants. Localization in the root of cation accumulation and of transfer to the shoot. Plant Physiol 17: 411–421
26. TORRI K, GG LATIES 1966 Mechanism of ion uptake in relation to vacuolation of corn roots. Plant Physiol 41: 863–870
27. TYREE MT, PG JARVIS 1982 Water in tissues and cells. *In* OL Lange, PS Nobel, CB Osmond, H Ziegler, eds, Physiological Plant Ecology, II. Water Relations and Carbon Assimilation, Encyclopedia of Plant Physiology, New Series, Vol 12B, Springer Verlag, Berlin
28. VAN VOLKENBURGH E, RE CLELAND 1980 Proton excretion and cell expansion in bean leaves. Planta 148: 273–78.
29. ZSOLDOS F, B KARVALY 1978 Effects of Ca^{++} and temperature in K^+ content distance along root of wheat, rice and cucumber. Physiol Plant 43: 331–336